



Cite this: *RSC Sustainability*, 2026, **4**, 1009

## Recovery of terephthalic acid from solar PV backsheets using waste solvent from distilled spirits production

Preeti Nain, <sup>a,b</sup> Elanna P. Neppel, Richard-Joseph L. Peterson, W. Aaron Davis, Nicole E. Shriner <sup>c</sup> and Annick Ancia <sup>a</sup>

Current research on solar photovoltaic (PV) recycling mainly focuses on recovering valuable metals and glass, often neglecting the polymeric components, particularly the backsheets, which are typically landfilled or thermally decomposed. This study explores an innovative approach to upcycle PV backsheets into value-added products, specifically terephthalic acid (TPA), using waste ethanol solvent from the distilled spirits industry. Experimental results show that increasing both exposure time and ethanol concentration significantly enhances backsheet delamination efficiency. Using waste ethanol, a maximum delamination efficiency of 80% was achieved at room temperature after 24 hours. In decomposition trials, both sodium hydroxide (NaOH) and potassium hydroxide (KOH) demonstrated comparable efficiencies (96.6–97.5%) over 8 and 24 hour reactions. With virgin ethanol, NaOH yielded 94–97.5% TPA recovery. Notably, using waste ethanol achieved a TPA recovery efficiency of 96.8%, underscoring the process's economic viability and sustainability. Analytical characterization of TPA recovered after 8 hours showed consistent spectral patterns across both alkalis and solvents, indicating a similar chemical environment and functional groups. The recovered TPA can be repolymerized into high-purity PET, suitable for manufacturing new PV backsheets. This work advances polymer-recycling by demonstrating that an industrial waste solvent (distilled-spirits 'heads') can replace virgin ethanol without loss in delamination performance or TPA yield. While PV backsheets PET is a modest share of global PET, using waste ethanol to upcycle this currently under-recycled stream demonstrates a transferable solvent-reuse pathway that can extend to higher-volume PET sources.

Received 10th July 2025  
Accepted 31st December 2025

DOI: 10.1039/d5su00581g  
[rsc.li/rscsus](http://rsc.li/rscsus)



### Sustainability spotlight

To support clean energy goals, sustainable recycling of solar PV materials is essential. This research spotlights an innovative approach to upcycling polymeric backsheets from end-of-life crystalline silicon solar modules into terephthalic acid (TPA), a valuable precursor for new PET materials. By comparing virgin ethanol and waste ethanol (from alcoholic beverage distillation) as green solvents, the study demonstrates an environmentally responsible method to delaminate and recover PET. Utilizing waste solvents not only reduces reliance on virgin chemicals but also advances circular economy principles. This work contributes to building a sustainable solar PV recycling ecosystem through green chemistry and high-value material recovery.

## 1. Introduction

With the rise in global energy demand and the ongoing green energy transition, solar photovoltaic (PV) installations have experienced exponential growth, with cumulative capacity now exceeding 1 terawatt.<sup>1</sup> Many of the crystalline silicon PV modules installed in the early 2000s are approaching the end of

their service life, and it is estimated that the United States alone will generate approximately 1.1 billion end-of-life modules by 2030.<sup>2</sup> Extensive research has focused on recycling these crystalline silicon modules, primarily targeting the recovery of valuable metals and glass.<sup>3,4</sup> Current recycling methods typically employ thermal treatment or organic solvents to break down encapsulants and separate the layers of the module. However, these approaches often leave behind polymeric waste, particularly the backsheets, which are either discarded without further treatment or subjected to pyrolysis or combustion.<sup>5</sup>

From a circular economy perspective, it is essential to recycle PV backsheets along with other module components. This not only enables the recovery of materials such as polyethylene terephthalate (PET) but also helps prevent the release of

<sup>a</sup>Civil and Environmental Engineering, Michigan State University, East Lansing, 48824, USA. E-mail: [nainp@ornl.gov](mailto:nainp@ornl.gov)

<sup>b</sup>Manufacturing Energy Efficiency Research and Analysis Group, Oak Ridge National Laboratory, Oak Ridge, TN, USA

<sup>c</sup>Chemical Engineering and Material Science, Michigan State University, East Lansing, 48824, USA

microplastics into the environment.<sup>6</sup> As the volume of decommissioned PV modules continues to rise, the development of sustainable and efficient recycling strategies for backsheets becomes increasingly critical.

One of the primary challenges in PV recycling lies in the encapsulated structure of modules.<sup>7</sup> The active semiconductor layer is tightly sandwiched between a glass front and a polymeric backsheets using ethylene-vinyl acetate (EVA), which ensures durability under harsh environmental conditions and long-term operational stability.<sup>8</sup> Efficiently separating these layers without any damage is the prerequisite for successful PV recycling. Various physical and chemical techniques have been explored to achieve intact separation of PV layers, with most research efforts focused on the recovery of valuable metal components.<sup>9,10</sup> In contrast, the recycling of the polymeric backsheets, particularly through environmentally friendly methods, has received comparatively little attention. It is mainly due to the complex composite nature of the backsheets.<sup>11</sup> Developing a green and efficient method for separating and upcycling PV backsheets into value-added products with minimal environmental impact could significantly advance the solar PV recycling industry.

Previous studies have explored pyrolysis-catalytic approaches to convert PV plastic waste into useful products such as syngas or carbon-based nanomaterials.<sup>5,12</sup> However, current treatment methods often rely on hazardous organic solvents like toluene, benzene, and trichloroethylene,<sup>13</sup> or involve energy-intensive thermal processes.<sup>14</sup> Only a limited number of studies have investigated the use of greener solvents, such as ethanol, to recycle PV backsheets materials like PET.<sup>15</sup> While ethanol is considered an environmentally friendly solvent, existing research typically utilizes commercially available virgin ethanol. There remains a critical need to explore the reuse of waste organic solvents from other industries as an alternative, sustainable approach to recycling polymeric PV waste, offering both environmental and economic benefits.

Waste ethanol is produced as a by-product during the distillation of spirits. In batch distillation, the distillate is typically divided into three fractions: the heads, hearts, and tails. Only the hearts fraction is retained as the desired product for commercial sale. The heads fraction, also known as the foreshot, is an unwanted by-product that contains not only ethanol but also methanol, aldehydes, and other toxic compounds.<sup>16</sup> Due to its toxicity and the presence of off-flavors, the heads fraction is unsuitable for use in consumable alcoholic beverages.<sup>17</sup>

In 2023, the United States produced approximately 2.7 billion liters of distilled spirits.<sup>18</sup> Based on an estimated yield of 1.5 liters of heads per hectoliter of low wines in a typical batch distillation process,<sup>17</sup> this corresponds to nearly 100 million liters of heads distillate generated annually. The heads fraction contains ethanol plus methanol, aldehydes, and other congeners and is unsuitable for beverage use. Industry handling pathways include increasing the ratio of product to heads<sup>19</sup> and exploring alternative uses such as redistillation/recovery,<sup>20,21</sup> blending with fermented wort,<sup>20,22</sup> and energy recovery *via* combustion.<sup>23</sup> When reuse is not feasible, the heads fraction

may be managed as process waste in accordance with local regulations.<sup>24,25</sup> However, the extent to which the heads can be reused varies significantly depending on the specific distillation system and process conditions.

A sustainable approach is proposed for the reuse of waste ethanol heads, byproducts from the distilled spirits industry, as an alternative to virgin ethanol in the green separation and recycling of solar PV backsheets. While previous studies<sup>13–15</sup> have examined the relationship between alcohol concentration and EVA swelling behavior, the reuse of industrial waste ethanol has not been established or benchmarked against virgin ethanol across a controlled process window. The novelty of the present approach lies in the integration of the following two unique aspects: (i) the use of industrial waste ethanol (specifically the “heads” fraction from distilled spirits production) as a sustainable solvent alternative and (ii) a systematic comparison of delamination efficiencies across a wide ethanol concentration gradient (25–100%) under varying thermal conditions (room temperature, 60 °C, and reflux).

Beyond ethanol, several greener solvents relevant to PET recycling are emerging. Bio-based polar aprotic solvents and deep eutectic solvents derived from bio-phenols can mediate alkaline hydrolytic depolymerization of PET under comparatively mild conditions (<150 °C, ≤5 h) with >90% TPA recovery and solvent reuse. In parallel, solvent choices used in circular separations are also greening; for example, γ-butyrolactone was employed to fabricate chemically recyclable nanofiltration membranes, illustrating how greener solvents can support closed-loop processing infrastructure that interfaces with polymer recycling.<sup>26</sup> In our case, the use of waste-derived ethanol aligns with these trends by leveraging a low-toxicity, readily recoverable, and waste-valorizing solvent, advancing green solvent use for PV backsheets recycling.

Unlike prior studies that typically used virgin solvents under narrow conditions or theoretical models of swelling, this study provides empirical evidence demonstrating the delamination performance and equilibrium swelling behavior of EVA using a waste-derived solvent. Further, the recovered TPA can be repolymerized into high-purity PET,<sup>27</sup> which is suitable for use in the production of new PV backsheets. This holistic, cross-industry waste valorization approach not only advances green PV recycling but also informs solvent reuse strategies across sectors. The recovered TPA can be repolymerized into high-purity PET,<sup>27</sup> which is suitable for use in the production of new PV backsheets. Positioned within recent advances in plastic upcycling, our solvent-substitution strategy complements catalytic and process-intensification approaches by reducing virgin solvent inputs while maintaining TPA quality.<sup>28</sup>

This study uses a combination of mechanical and chemical approaches to upcycle the backsheets of crystalline silicon solar modules into TPA. Specifically, it compares the efficiency of PV backsheets delamination and TPA recovery using two different solvents: commercially available virgin ethanol and waste ethanol derived from the distillation of alcoholic beverages. In this work, “waste” strictly means “not returned to beverage production” and does not imply landfill disposal of distilled spirits. By utilizing waste ethanol in the recovery of PET from



end-of-life PV backsheets, this research offers a sustainable pathway for enhancing resource efficiency in the PV recycling industry. Further, we scope our contribution relative to the PET market size by quantifying expected PV polymer tonnages and explicitly positioning our method as complementary to packaging-scale recycling.

The present work is relevant for PV end-of-life because polymeric components are frequently neglected relative to glass and metals. By directly validating waste-ethanol performance against virgin ethanol across concentration and temperature regimes and demonstrating high TPA yield and purity, we show a practical route to upcycle two underutilized waste streams at once (PV backsheets and distillation heads), lowering solvent footprint and avoiding virgin solvent procurement.

## 2. Methods

The methodology overview of the present study is shown in Fig. 1.

### 2.1. Module dismantling and backsheets delamination

A multi-crystalline silicon solar module (specifications shown in Table S1) with a typical glass-backsheet design is purchased online from Amazon. A typical crystalline silicon PV module consists of multiple layers in the following order (from top to bottom): a protective glass front sheet, an encapsulant layer (EVA), crystalline silicon solar cells, a second EVA layer, and a polymeric backsheets. The schematic was shown in one of the previous papers by the author's group.<sup>29</sup> A handheld circular saw was used to detach the aluminum frame physically, and the junction box was manually scraped from the backsheets. The complete module was reduced to  $2 \times 2 \text{ cm}^2$  pieces using a waterjet and manual cutting.

The  $2 \times 2 \text{ cm}^2$   $20 \pm 1$  module pieces (weighing  $20 \pm 1$  grams) were submerged in 100 mL ethanol in a 250 mL beaker (for reactions at room temperature), and glass lid-enclosed jars (for reactions at  $60^\circ\text{C}$  temperature and above) were placed in an oil bath. As the boiling point of ethanol is  $78^\circ\text{C}$ , the reactions

above it ( $80 \pm 2^\circ\text{C}$ ) were considered reflux. No water-cooled reflux condenser equipment was used. After a few hours of immersion, the adhesion between EVA and glass loosened. The module pieces were removed and air-dried for 5 minutes, and the backsheets was manually removed using a scalpel after sufficient swelling of the EVA layer was observed. While the swelling process weakened the adhesion between EVA and the glass/backsheet interface, complete detachment did not occur spontaneously in all cases. Manual intervention ensured consistent separation, especially under suboptimal conditions such as lower ethanol concentration or shorter exposure times.

The impact of three variables was investigated on backsheets delamination: (i) reaction time (submergence time of module pieces in ethanol, 1 h to 5 h), (ii) temperature (RT,  $60^\circ\text{C}$ , and reflux), and (iii) ethanol concentration (25%, 50%, 75%, 85%, and 100%).

The backsheets separation/delamination efficiency was calculated as per eqn (1).

$$\text{Delamination efficiency}(\%) = \frac{n}{N} \times 100 \quad (1)$$

where,  $N$  denoted the total number of PV pieces taken initially, and  $n$  denoted the number of PV pieces from which the backsheets can be separated after submergence in ethanol.

To assess the change in ethanol concentration throughout the experiments, 100 mL of ethanol was poured into a 250 mL beaker (for reactions at room temperature) or 250 mL glass lid-enclosed jars (for reactions at  $60^\circ\text{C}$  temperature and above) and was placed in an oil bath. After each hour, a sample was removed and cooled to room temperature. The alcohol by volume (ABV) was determined using an EasyDens Digital Density Meter (Anton Paar, Graz, Austria). The experiment was repeated for ethanol concentration (25%, 50%, 75%, 85%, and 100%) and temperature (RT,  $60^\circ\text{C}$ , and reflux). The 100 mL of various ethanol concentrations were prepared using volumetric flasks, and the respective concentration was confirmed using the EasyDens. Unless otherwise noted, ethanol concentrations

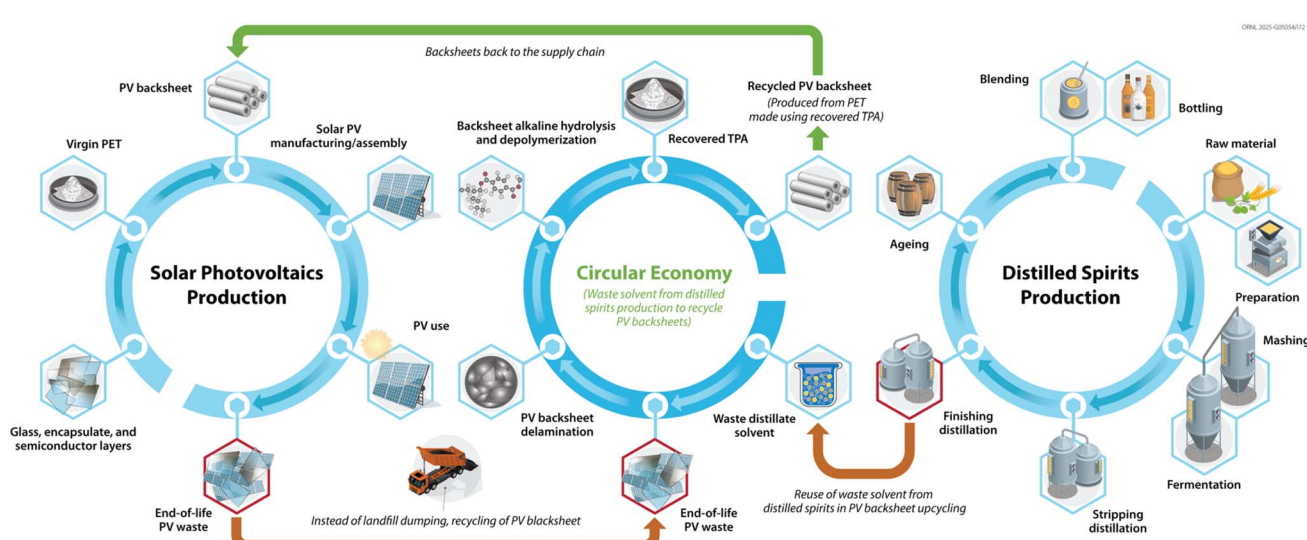


Fig. 1 Methodology overview of the present study.



refer to v/v ethanol–water mixtures prepared by diluting ethanol with distilled water in volumetric flasks to 25%, 50%, 75%, and 85% v/v; 100% ethanol (CAS #64-17-5) was used as received. The waste ethanol (~80% v/v ‘heads’ fraction, received from Dr Nicole Shriner lab from Michigan State University, East Lansing, USA) was used neat for the ~80% condition and, when needed, diluted with distilled water to reach the desired concentration.

## 2.2. Alkaline hydrolysis and depolymerization

The alkaline hydrolysis of the recovered backsheet was conducted using two alkalis (NaOH and KOH), two ethanol types (virgin ethanol and waste ethanol), and four reaction times (1 h, 4 h, 8 h, and 24 h). All reactions were performed using standard ethanol. Based on PV backsheet decomposition and TPA recovery experiments, the reaction was performed again using waste ethanol from distilled spirits production for the best combination. The reaction method for TPA recovery from solar module backsheets was illustrated in Fig. 2.

Using a 100 mL stainless steel cup equipped with a stir bar (300 rpm),  $1.25 \pm 0.02$  g NaOH ( $31.3 \pm 0.5$  mmol) or  $1.75 \pm 0.06$  g KOH ( $31.2 \pm 1.1$  mmol) pellets were dissolved in 15 mL of anhydrous ethanol (no added water). Once dissolved, 1 g of separated PV backsheet was added at  $40^\circ\text{C}$ . Stainless steel reactor cup was chosen for mechanical robustness and compatibility with ethanolic alkaline media at  $40^\circ\text{C}$ ; borosilicate glassware can be used interchangeably for this procedure. The stoichiometric basis for PET alkaline hydrolysis is explained in the SI Document.

The same total ethanol volume (15 mL) was used for all depolymerization experiments, irrespective of ethanol source. The waste ethanol (‘heads’ stream) contained ~80% v/v ethanol with trace co-volatiles (e.g., methanol and esters) at ppm levels by GC (Fig. S1). No volumetric correction was applied for these

impurities because reactions were run with a large excess of solvent and hydroxide relative to the PET ester content (standard charge: 1.25 g NaOH in 15 mL solvent per 1 g backsheet), which renders minor variations in ethanol composition inconsequential to reaction stoichiometry and kinetics.

Reactions were stopped at 1, 4, 8, and 24 hours by quenching the reaction with 30 mL of distilled water. Then, the resulting mixture was filtered using ordinary filter paper to remove any remaining unreacted or undecomposed back sheet. The supernatant was then acidified using 12 M hydrochloric acid to a pH of 4, causing the TPA to drop out of solution. The resulting TPA was rinsed and collected through filtration and dried in a convection oven at  $100^\circ\text{C}$  overnight. The mass of residues at each step was measured to calculate the backsheet decomposition efficiency (DE) for four reaction times (1 h, 4 h, 8 h, and 24 h) and two alkalis (KOH, NaOH) as per eqn (2).

$$\text{DE}(\%) = \frac{M - m}{M} \times 100 \quad (2)$$

where,  $M$  (g) denoted the total mass of the initial back sheet, and  $m$  (g) denoted the total mass of the undecomposed back sheet. The TPA recovered was also calculated based on the amount of PET in the backsheet using eqn (3).

$$\text{TPA}\% = \frac{T_{\text{actual}} - T_{\text{theoretical}}}{T_{\text{theoretical}}} \times 100 \quad (3)$$

where  $T_{\text{actual}}$  (g) is the amount of TPA recovered after acidification and  $T_{\text{theoretical}}$  (g) is the theoretical maximum amount of TPA that can be recovered based on the amount of PET in the backsheet. The amount of PET present in the backsheet was determined by reacting the backsheet until completion, which was defined operationally as no additional measurable mass loss after extended reaction. In practice, the backsheet samples were subjected to alkaline hydrolysis for at least three consecutive days, and mass was recorded daily. When no further

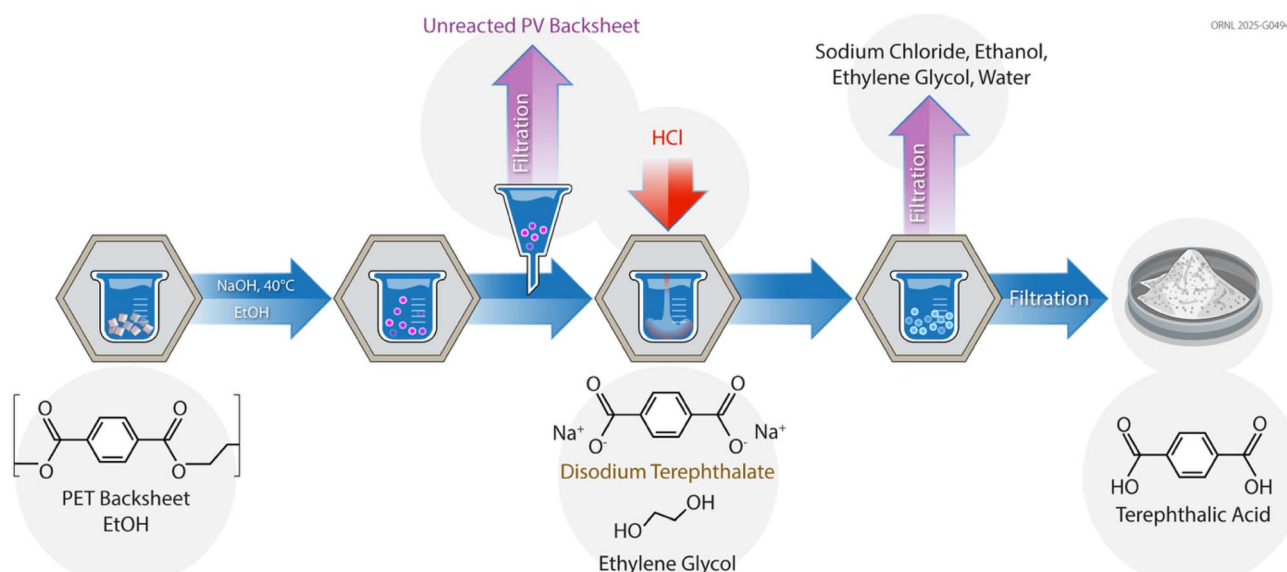


Fig. 2 Backsheet decomposition and TPA recovery process [Reagent: NaOH 1.25 g (31.3 mmol) or KOH 1.75 g (31.2 mmol) in 15 mL EtOH ( $\approx 2.08$  M)].



decrease in mass was observed over this period, the reaction was assumed to have gone to completion, indicating that all the PET had been depolymerized. The residual mass was then used to estimate the non-PET fraction of the backsheet.

### 2.3. Waste solvent from distilled spirits production

The waste solvent (or waste ethanol) with approximately 80% ethanol concentration was a by-product of distilled spirit production. The backsheet delamination and alkaline hydrolysis experiments were also performed using a waste solvent to show the feasibility of PV backsheet recycling using waste solvent instead of virgin ethanol. The distilled spirits production used fermentation of ten different grains, with two subsequent distillations. The waste solvent was the mixture of heads collected from the second distillation of each grain variety. The detailed distilled production process is provided in the SI.

## 2.4. Analysis and characterization

**2.4.1. Scanning electron microscopy and energy-dispersive X-ray (SEM/EDX) spectroscopy.** The backsheet samples were characterized using SEM (6610LV JEOL Ltd, Tokyo, Japan) and EDX (Oxford Instruments, High Wycomb, Bucks, England) to observe changes in morphology and elemental composition of the original backsheet, backsheet after hydrolysis, and recovered TPA.

**2.4.2. Attenuated total reflectance- fourier transform infrared (ATR-FTIR) spectroscopy.** To understand the intermolecular interaction and organic composition, the recovered TPA was characterized using Fourier-transform infrared spectroscopy (FTIR, Spectrum 100 equipment, PerkinElmer), with the spectral window of 4000–650 cm<sup>-1</sup>, and resolution of 4 cm<sup>-1</sup>. Intensities in the spectra obtained were normalized to one for comparison.

**2.4.3. Nuclear magnetic resonance (NMR) spectroscopy.** Using dimethylsulfoxide (DMSO) as a deuterated reagent, the proton Nuclear Magnetic Resonance (NMR, Bruker 500 MHz) spectra of recovered TPA from the PV backsheet were taken. The parameters used were 32 scans with a two-second relaxation delay. The concentration of the samples was around 20 mg mL<sup>-1</sup>. For each characterization method, standard TPA (Sigma-Aldrich) was used as a basis for comparison.

**2.4.4. Gas chromatography (GC).** GC was used to quantify the volatile composition of the waste solvent collective heads fraction distillate using a Shimadzu GC-17A instrument installed with a flame ionization detector and AOC-20i auto-injector (Shimadzu, Kyoto, Japan). The GC injector was set to split mode (25:1 split ratio) at 220 °C using helium as the carrier gas. The oven temperature started at 40 °C and ramped to 100 °C at 15 °C min<sup>-1</sup>, then to 230 °C at 25 °C min<sup>-1</sup>, where the final temperature was held for 6 minutes. The chromatograms were analyzed using EZStart 7.4 software (v. SP2, Shimadzu, Kyoto, Japan). All standards used for identification and quantification were purchased from Sigma-Aldrich. Calibration curves for each compound using at least 6 concentrations were established using 1,2-dimethoxyethane as the internal standard (ISTD). For each calibration level and sample analyzed, 0.9 mL

of solution was mixed with 0.1 mL of the internal standard in 1.5 mL GC vials and vortexed prior to analysis.

**2.4.5. Thermogravimetric analysis (TGA).** TGA was performed on a TA Instruments Q500. Samples included: (i) recovered terephthalic acid (TPA) from backsheet depolymerization using NaOH, KOH, and waste distilled solvent streams; (ii) a TPA standard (Fisher Scientific, >99.5% purity); and (iii) thermoform waste PET. Analyses were conducted under nitrogen purge (40 mL min<sup>-1</sup>). Each specimen was equilibrated at 50 °C, then heated to 500 °C at a constant rate of 10 °C min<sup>-1</sup>. Sample mass was recorded continuously as a function of temperature and time, and the resulting thermograms were exported for post-processing and comparison among samples.

**2.4.6. Analysis of variance (ANOVA).** The significant effect of different variables on PV backsheet delamination efficiency was analyzed using ANOVA in Minitab software. The impact was considered statistically significant at  $p \leq 0.05$ . The  $p$ -value and mean responses were compared for three parameters: temperature (RT, 60 °C, reflux), ethanol concentration (25%, 50%, 75%, 85%, and 100%), and time (1 h, 2 h, 3 h, 4 h, and 5 h).

## 3. Results and discussion

### 3.1. Backsheet delamination

EVA is a widely used copolymer resin known for its flexibility, elasticity, and lightweight properties. It is commonly employed as a sealant to bond the backsheet to semiconductor layers in various applications. In addition to its mechanical properties, EVA is also recognized for its excellent gas barrier performance, making it a popular choice in packaging industries.<sup>30</sup> Previous studies have demonstrated that EVA can undergo alcoholysis using short-chain alcohols (typically those containing 1–4 carbon atoms), with methanol being the preferred reagent.<sup>31</sup> This process converts ester groups into hydroxyl groups, resulting in the formation of ethylene-vinyl alcohol (EVOH) resin.

In the current study, alcoholysis was used as a method to dissolve EVA. The effectiveness of this process is highly influenced by the vinyl acetate content in the EVA. EVA with a higher vinyl acetate content tends to swell extensively<sup>32</sup> and can be separated when treated with organic solvents such as xylene or chloroform, provided that no additives (e.g., plasticizers) are present in the polymer.<sup>33</sup> Comprehensive information on the swelling and separation behavior of EVA is available in a recent study by Trivedi *et al.* (2023).<sup>34</sup>

Before evaluating the effectiveness of water/ethanol mixtures for backsheet delamination, it is essential to first understand how the ethanol concentration evolves over time. Mixtures with initial ethanol concentrations of 25%, 50%, 75%, 85%, and 100% were studied under three temperature conditions: room temperature, 60 °C, and under reflux. At room temperature and 60 °C, the ethanol concentrations remained largely stable across all mixtures. However, under reflux conditions, notable changes were observed depending on the initial ethanol content. As shown in Fig. 3, mixtures with lower starting ethanol concentrations exhibited a more significant reduction in alcohol by volume (ABV) over time.



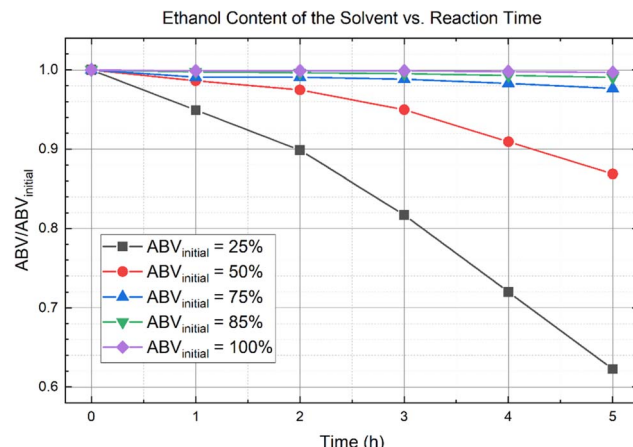


Fig. 3 Change in ethanol concentration with time at reflux.

In contrast, mixtures with initial concentrations of 75%, 85%, and 100% ethanol showed minimal change even after 5 hours of reflux, while those with 50% and 25% ethanol experienced substantial ethanol loss, indicating a preferential evaporation of ethanol. This behavior can be explained by the shift in vapor–liquid equilibrium as the composition of the mixture changes (see Fig. S2 in the SI). As the ethanol content increases, the boiling point of the mixture decreases, and the system approaches the azeotropic point, where ethanol and water vaporize together in a fixed ratio. However, at lower ethanol concentrations, the boiling point increases, approaching that of pure water. In these conditions, ethanol, being more volatile, tends to concentrate in the vapor phase, leaving behind a more water-rich liquid. Consequently, mixtures with lower ethanol content undergo more pronounced composition shifts over time due to this preferential evaporation, while mixtures with higher ethanol concentrations (75% and above) remain relatively stable.

In this study, the swelling behavior of EVA was observed after several hours of immersion in ethanol. The swelling generated internal pressure between the silicon wafer and the backsheet, leading to mechanical stress that damaged the silicon wafer and caused edge separation. The backsheet was manually detached using tweezers, and the swollen EVA layer was peeled off the surface.

The dissolution of cross-linking in EVA and the efficiency of backsheet separation were investigated under varying ethanol concentrations and temperatures. As shown in Fig. 4, delamination efficiency was assessed across varying ethanol concentrations and temperatures. After 5 hours at room temperature, ethanol concentrations ranging from 25% to 85% yielded a maximum separation efficiency of 10%. In contrast, immersion in pure ethanol improved delamination performance, reaching 55% efficiency after 5 hours. Complete delamination (100% efficiency) was achieved after 24 hours, though theoretically, the swelling necessary to achieve 100% delamination efficiency occurred much sooner. Assuming a linear relationship, the projected time to reach full delamination was estimated to be just under 10 hours.

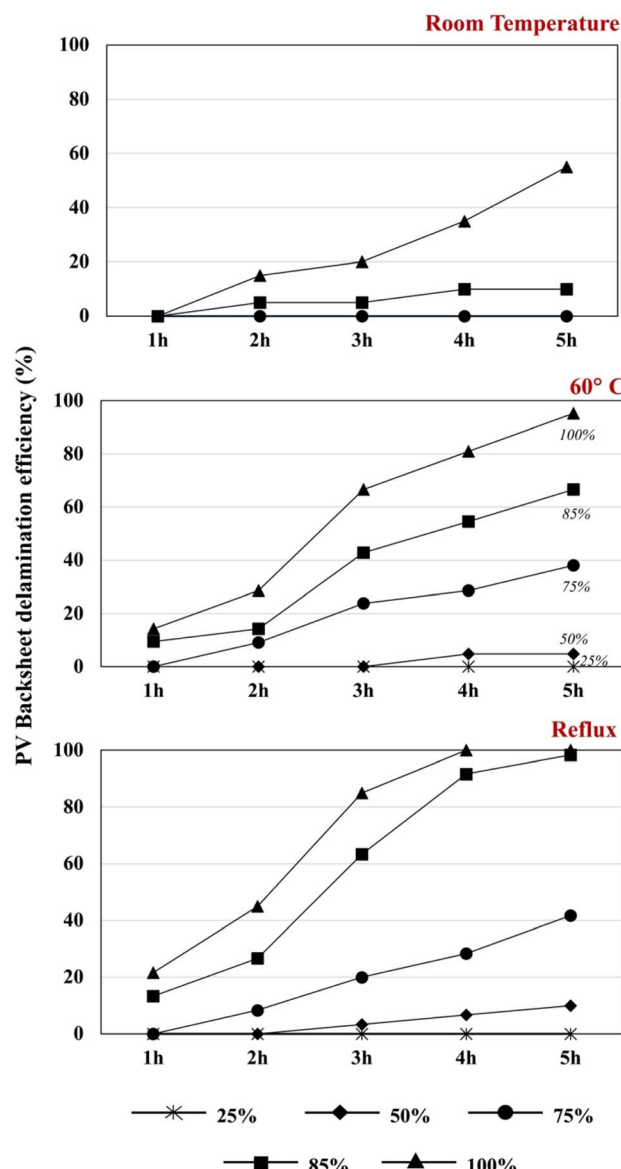


Fig. 4 The effect of ethanol concentration (25%, 50%, 75%, 85%, and 100%) and temperature (room temperature, 60 °C, reflux) on the separation efficiency of the backsheet.

The delamination efficiency observed with 85% ethanol at room temperature can be used to estimate the time required to achieve complete (100%) delamination. Assuming a linear relationship between delamination efficiency and time, it is projected that full delamination of the backsheets would occur in approximately 40 hours, based on the observation that 10% efficiency was achieved in 4 hours. This result indicates that the swelling rate is highly dependent on ethanol concentration.

Not only is the swelling rate a function of concentration, but so is equilibrium swelling. Chuang *et al.* examined the equilibrium swelling behavior of EVA in water/ethanol mixtures and found that at 37 °C, pure ethanol caused EVA to swell 1.8 times more than an 85% water/ethanol mixture.<sup>35</sup> Additionally, a 25% ethanol solution resulted in 5.8 times less swelling than pure ethanol. In a related study, Chen *et al.* investigated equilibrium



swelling at 25 °C as a function of both ethanol concentration and vinyl acetate content.<sup>36</sup> They observed that for all vinyl acetate levels, equilibrium swelling approximately doubled as ethanol concentration increased from 75% to 100%. These findings highlight the strong dependency of equilibrium swelling on ethanol concentration. As a result, it is likely that at room temperature, low concentrations of ethanol may be insufficient to cause delamination of a multi-layered PV backsheet.

Increasing the solvent temperature enhances both the swelling rate and the equilibrium swelling of the material. At 60 °C, the swelling rate in pure ethanol nearly doubles, achieving over 90% delamination efficiency within 5 hours. A similar trend is observed for water/ethanol mixtures, where the swelling rate increases with temperature. Assuming a linear correlation between delamination efficiency and time, 85% and 75% ethanol mixtures are projected to reach 100% delamination efficiency after 7.5 hours ( $R^2 = 0.968$ ) and 12 hours ( $R^2 = 0.958$ ), respectively. Interestingly, while 50% and 75% ethanol mixtures show no delamination at room temperature, delamination does occur after 5 hours when the temperature is raised to 60 °C or higher. This indicates that the equilibrium swelling increases for lower ethanol concentrations as the temperature rises.

To maximize the swelling rate and thereby minimize the delamination time, the oil bath temperature was increased to the reflux point of each ethanol concentration. Reflux data, averaged over three replicates (see Fig. S2 in the SI), were collected with the oil bath heated above the boiling point of each water/ethanol mixture. The boiling point varies with ethanol concentration, ranging from 78.37 °C for pure ethanol to approximately 82 °C for a 25 mol% ethanol mixture. As shown in Fig. 4, reflux conditions led to reduced delamination times for pure ethanol and 85% ethanol mixtures, with no significant improvement observed for the 75% mixture. This may be attributed to ethanol in the 75% mixture already reaching near-reflux conditions at 60 °C. For the 50% and 25% ethanol mixtures, the limited improvement in delamination under reflux is likely due to solvent loss through evaporation, which reduces the effective ethanol concentration in the mixture (as illustrated in Fig. 4 and discussed above).

It is important to recognize that the EVA swelling and backsheet delamination behavior vary between solar modules from different manufacturers. Under identical experimental conditions, RT exposure to 100% ethanol, a monocrystalline silicon module from Renogy exhibited only partial delamination, with a maximum of 40% backsheet separation observed after 24 hours. In contrast, the same treatment applied to a multi-crystalline silicon module resulted in complete delamination within the same time frame. This variation is largely attributed to differences in the EVA composition, particularly the vinyl acetate (VA) content, which influences swelling behavior in ethanol. Since the delamination rate is governed by the swelling rate of EVA, modules with slower delamination likely contain a lower VA content.

EDX analysis of the mono-Si module (Fig. S3, SI) revealed the presence of fluorine in the backsheet. This suggests the

manufacturer may have selected a lower VA content in the EVA to enhance adhesion with the fluoropolymer-based backsheet. Ultimately, the rate of backsheet delamination depends on a combination of factors, including EVA formulation, PV module type, and backsheet material, all of which vary by manufacturer. The lack of transparency regarding material composition by PV manufacturers further complicates the efficient recycling of all solar module components.

The ANOVA analysis was conducted to evaluate the significant effects of temperature, ethanol concentration, and exposure time on PV backsheet delamination (Fig. 5). Among the variables studied, ethanol concentration exhibited the highest mean response, followed by time and temperature. The response range varied from 0–60% for ethanol concentration, 10–50% for time, and 20–40% for temperature. These findings indicate that increasing ethanol concentration from 25% to

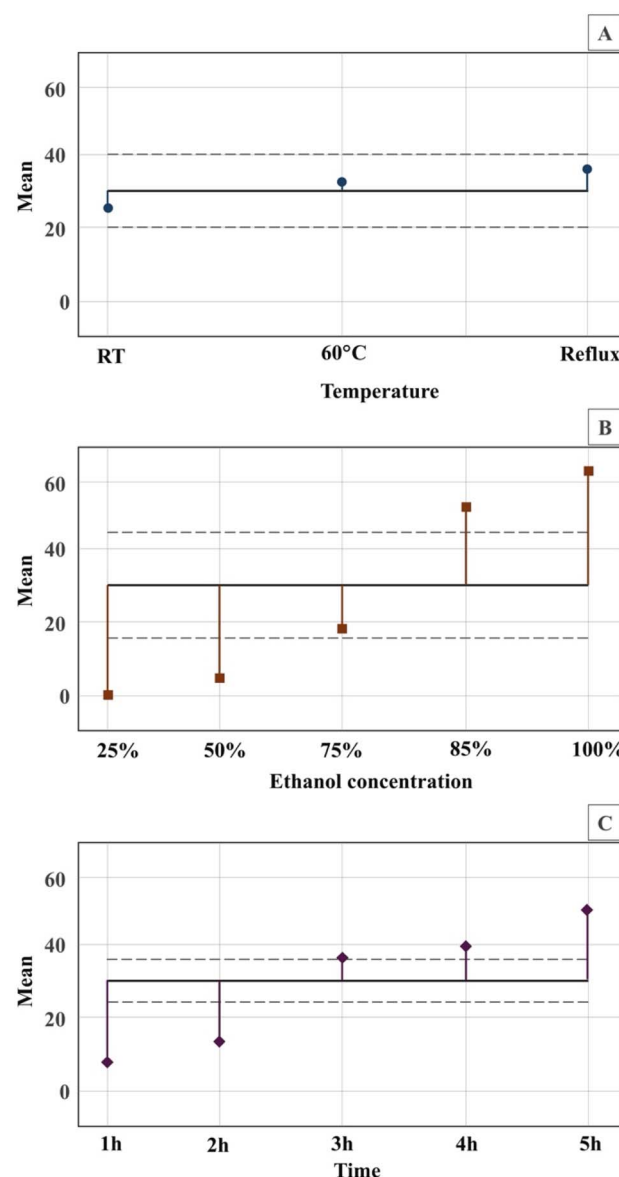


Fig. 5 Mean effect of (A) temperature, (B) ethanol concentration, and (C) time on delamination efficiency of the PV backsheet.



100% had the most pronounced effect on backsheet delamination, with time and temperature having progressively lesser impacts.

An additional factor that may influence the delamination rate is the solid-to-liquid ratio (*i.e.*, the proportion of PV material to ethanol volume), which warrants further investigation in future studies. Previous research has also highlighted the role of solvent type in polymer degradation.<sup>9,13</sup> Intermolecular interactions between EVA and organic solvents can disrupt the intramolecular bonds within polymer chains, creating free volume that leads to swelling and eventual delamination of the laminated structure.<sup>34</sup> Chlorine-containing solvents, such as chloroform, are known to interact more strongly with EVA. According to Hansen solubility parameters, EVA with 33% vinyl acetate content is much less soluble in ethanol compared to chlorinated solvents.<sup>37</sup> Nevertheless, greener alternatives such as pure ethanol and ethanol-based waste byproducts have demonstrated sufficient swelling capability to enable delamination of EVA backsheets in multi-Si modules.

When utilizing waste ethanol derived from distilled spirit production for backsheet delamination, a maximum efficiency of 80% was achieved after 24 hours at RT (Fig. 6). Based on a linear regression model ( $R^2 = 0.891$ ), the projected time required for complete delamination is approximately 33 hours. Compared to pure ethanol, the use of 80% ethanol head cut resulted in a threefold increase in delamination time at RT. Although limited data were available for 85% ethanol at RT, the estimated delamination time was around 40 hours. These findings suggest that 80% waste ethanol exhibits a delamination performance comparable to that of commercially available 80% ethanol solutions.

Given that 80% waste ethanol derived from the distillation of spirits exhibits similar behavior to pure 80% ethanol, its delamination behavior at elevated temperatures can be reasonably extrapolated. For estimation purposes, the delamination time for 80% ethanol is assumed to be the average of the delamination times observed for 85% and 75% ethanol solutions. Based on this approach, the projected delamination times for the waste ethanol are approximately 9.7 hours at 60 °C

and 8.6 hours under reflux conditions. These results suggest that the waste ethanol will induce sufficient swelling in EVA to achieve full backsheet delamination at a rate roughly twice as slow as that of pure 100% ethanol.

GC was used to determine the volatile composition of the ethanol waste solvent, not only measuring the concentration of ethanol but also other minor component compounds that may be present. A sample GC report of the volatile profile is provided in the SI (see Fig. S1). Although compounds such as methanol and other alcohols were detected, the presence of such impurities was in concentrations of ppm, thus negligible in their effect on delamination. Concentration ranges from 25 to 5000 ppm were used to establish the GC calibration curves, applying a linear fit and ensuring a minimum  $R^2$  value of 0.995. Due to the high concentration of ethanol, ethanol was tested up to the saturation limit of the individual FID detector and the method. Additional runs using diluted samples were also completed to confirm the determined concentration of the “waste” ethanol.

Up to 80% backsheet delamination was achieved within 24 hours at RT. The waste solvent, a byproduct of distilled spirits production, contained approximately 80% ethanol. The presence of additional alcohols in the mixture may further enhance delamination efficiency, particularly when the process is conducted at elevated temperatures (50 °C or 60 °C) and with a higher solid-to-liquid ratio. These findings highlight the need for future studies to explore the effects of key variables, such as different PV module types from different manufacturers and processing temperatures, on the effectiveness of backsheet delamination.

### 3.2. Backsheet decomposition

Fig. 7A illustrates the decomposition efficiency of the PV backsheet under varying reaction times, types of alkalis, and ethanol solvents. As reaction time increased, decomposition efficiency improved significantly under all conditions, approaching 100%. After 24 hours, both NaOH and KOH demonstrated comparable efficiencies, ranging from 96.6% to 97.5%. However, at shorter reaction times (2, 4, and 8 hours), KOH resulted in lower decomposition efficiencies compared to NaOH. Specifically, KOH achieved only 22.4% efficiency at 1 hour but rapidly increased to 81.4% at 4 hours and 99.1% at 8 hours. In contrast, NaOH showed 37.6% efficiency at 1 hour and exceeded 94% at all subsequent time points. By the 24 hour mark, both alkali treatments yielded nearly identical decomposition performance.

When waste ethanol was used as a substitute for virgin ethanol in the backsheet-CH<sub>3</sub>CH<sub>2</sub>OH-NaOH reaction system for PV backsheet decomposition, a decomposition efficiency of 96.3% was achieved after 8 hours (Fig. 7A, blue bar). The efficiency was only 1.2% lower than that obtained with standard (virgin) ethanol, indicating minimal loss in performance. This result suggests that ethanol recovered from spirits distillation can serve as an effective alternative to standard ethanol, with no significant difference in backsheet decomposition efficiency.

Fig. 8 presents SEM-EDS images of the solar module surface before and after hydrolysis.

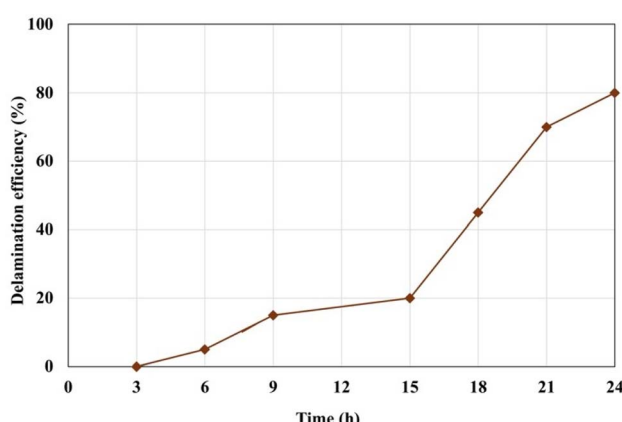


Fig. 6 Delamination efficiency for a multi-Si module in waste ethanol from the distillation of spirits (the heads cut).



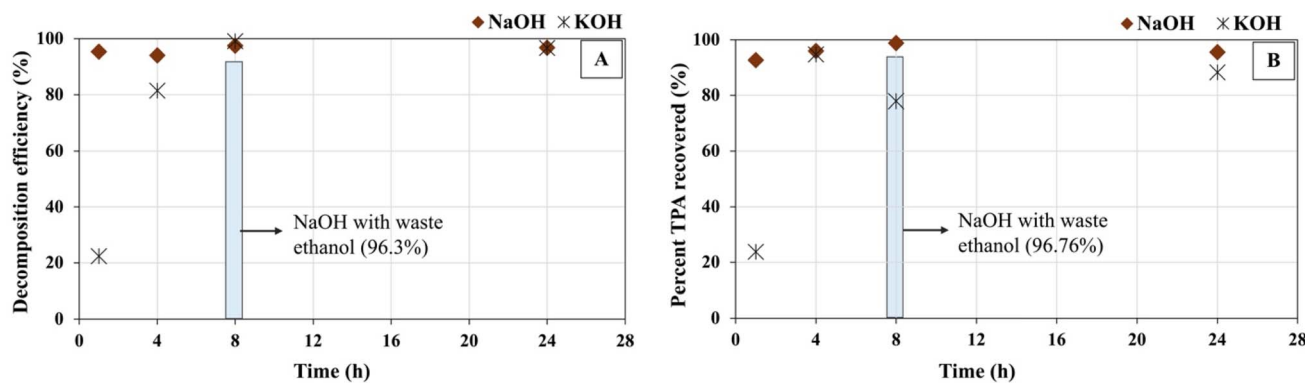


Fig. 7 Decomposition efficiency of PV backsheet (A) and TPA recovery from PV backsheet (B) for 1 h, 4 h, 8 h, and 24 h reaction times for three conditions: (i) NaOH with standard ethanol, (ii) KOH with standard ethanol, and (iii) NaOH with waste ethanol.

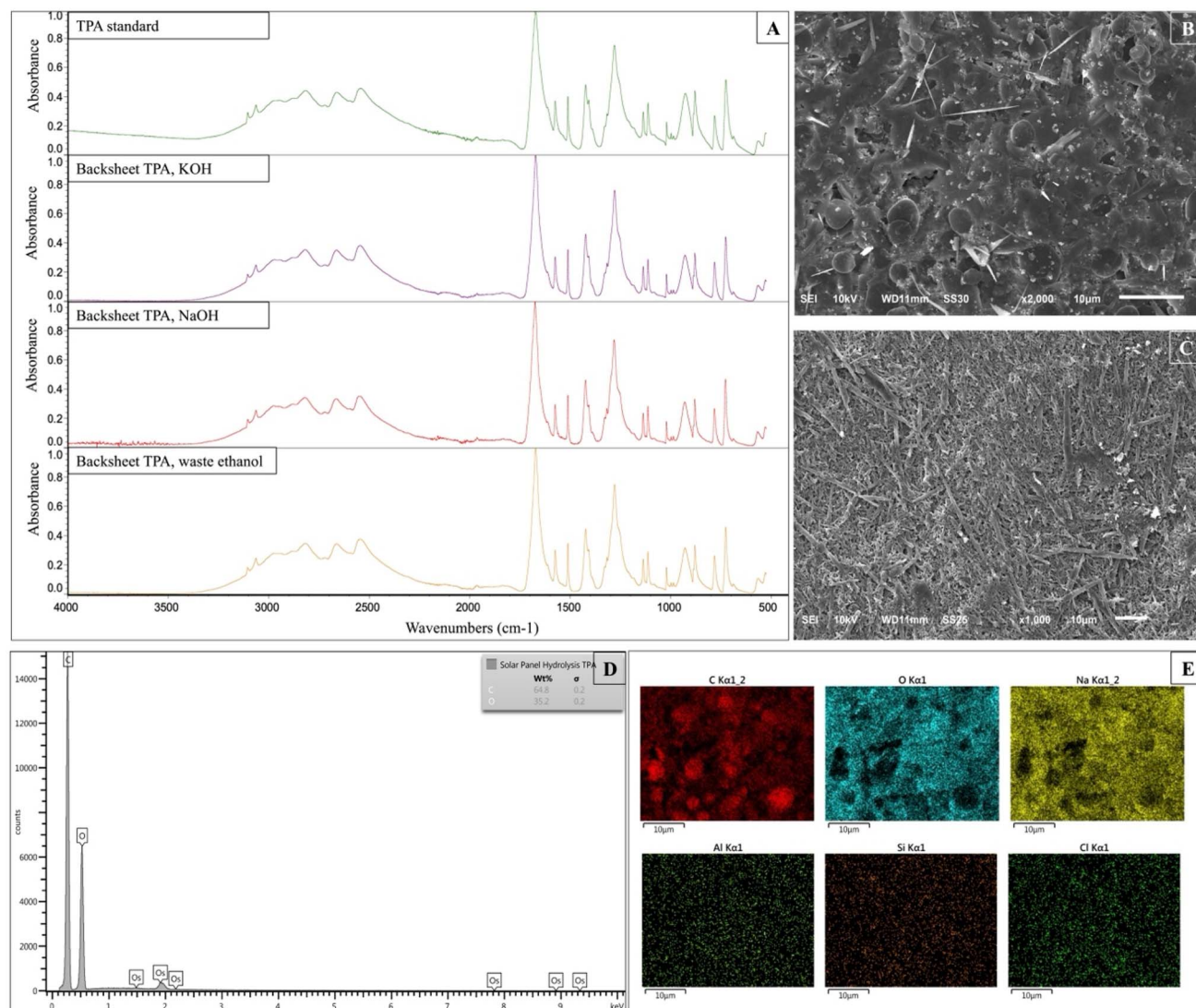


Fig. 8 (A): FTIR spectrum of standard TPA and recovered TPA from PV backsheet using KOH, NaOH, and NaOH using the heads; (B): SEM image of PV backsheet surface after hydrolysis; (C): SEM image of TPA obtained using NaOH; (D): EDS of PV backsheet surface after hydrolysis; (E): SEM images after hydrolysis, highlighting the locations showing where each type of atom is most present.



Prior to hydrolysis, the surface composition is measured at 73.3 wt% carbon and 26.5 wt% oxygen, corresponding to 78.7 mol% carbon and 21.3 mol% oxygen. Excluding the hydrogen atoms in the PET backbone, the theoretical composition of pure PET is approximately 71.4 mol% carbon and 28.6 mol% oxygen (based on a repeating unit containing 10 carbon atoms and 4 oxygen atoms). The slightly higher carbon content observed suggests the presence of additives or copolymers incorporated to improve material properties. The surface appears uniform before hydrolysis, indicating it is composed primarily of a single material, in this case, PET. Peaks labeled as 'Os' are attributed to the heavy metal coating used during SEM-EDS analysis and are therefore excluded from the mass percentage calculations.

Following hydrolysis, the surface of the remaining backsheet exhibited noticeable heterogeneity in both texture and composition. EDS analysis (Fig. 8) revealed distinct regions enriched in either carbon or oxygen. It is important, however, to note that these two areas do not overlap. The oxygen-rich regions also contained elevated levels of sodium, suggesting the presence of a thin surface layer composed of either a terephthalate salt or residual sodium hydroxide. In contrast, the carbon-rich regions lacked both oxygen and sodium, indicating that unreacted backsheet material, likely in higher concentration in these areas, remains. This residual material is most likely a form of polyolefin, potentially present as a copolymer or as a distinct layer within the structure. Additionally, trace amounts of aluminum, silicon, and chlorine were detected, likely originating from the original PV module from which the backsheet was removed.

The role of ethanol in the backsheet decomposition process is primarily to act as a cosolvent that facilitates the dissolution of the alkali (NaOH or KOH) and helps in the effective dispersion of the polymer matrix, enhancing contact between the alkali and the PET component of the backsheet. However, the decomposition of PET is mainly driven by the alkaline hydrolysis reaction, where NaOH or KOH cleaves the ester bonds in the PET structure. In the TPA recovery step, the acidification of the filtrate was carried out using 12 M HCl, and approximately 8–10 mL of the acid was added dropwise until the pH reached 4. This pH range was chosen to ensure complete precipitation of TPA without redissolving it or forming side products.

### 3.3. Terephthalic acid recovery

The recovery of TPA and the residual backsheet following hydrolysis under various reaction conditions are compared in Fig. 7B. Among the two alkalis tested, NaOH consistently demonstrated higher conversion efficiency. After one hour of reaction, 60.7% of the potential TPA was recovered using NaOH, compared to only 23.8% with KOH. For both alkalis, TPA recovery increased with reaction time, reaching over 90% after four hours. However, a decline in recovery was observed at eight hours in the KOH run. This reduction may be attributed to variations in the size of the backsheet flakes, as smaller flakes provide a greater surface area for reaction, thereby accelerating the hydrolysis process.

Waste ethanol demonstrated performance comparable to commercially available virgin ethanol when NaOH was used as the base. After 8 hours of reaction time, a TPA recovery of 96.8% was achieved using waste ethanol, compared to 98.8% with store-bought ethanol. These results indicate that the type of ethanol, waste or virgin, has minimal impact on TPA recovery efficiency. Remarkably, the comparable recovery rate using waste ethanol, despite the presence of impurities such as ethyl acetate and other alcohols, highlights the potential for reusing waste solvents from distilled spirits in the recovery of TPA from solar PV backsheets.

Moreover, the quality of the recovered TPA was consistent across both ethanol sources, as confirmed by FTIR (Fig. 8A) and H-NMR (Fig. 9). The FTIR spectrum of the TPA obtained after 8 hours under each condition showed no discernible differences compared to the standard TPA. This included matching peaks in the fingerprint region, confirming that the molecular structure and functional groups remained unchanged regardless of the ethanol source. Characteristic peaks included a broad band at 2500–3000  $\text{cm}^{-1}$  corresponding to hydroxyl group stretching, a peak at 1650  $\text{cm}^{-1}$  from carbonyl stretching, and peaks around 3000–3200  $\text{cm}^{-1}$  attributed to aromatic C–H stretches. Additionally, aromatic C–C stretches were observed near 1500  $\text{cm}^{-1}$ . No deviations were found between the spectra of standard TPA and TPA synthesized using waste ethanol, reinforcing the suitability of this recycled solvent for high-purity TPA recovery.

EDS analysis of the recovered TPA (Fig. 8D) reveals a composition of 64.8 wt% carbon and 35.2 wt% oxygen, corresponding to 71.0 mol% carbon and 29.0 mol% oxygen. For pure TPA, which contains 8 carbon atoms and 4 oxygen atoms per molecule, the expected molar composition is 66.7% carbon and 33.3% oxygen. The observed carbon content is therefore slightly higher than anticipated.

This deviation is partially expected, as the original PET backsheet exhibited a marginally higher carbon-to-oxygen ratio than the theoretical value. Several factors may contribute to the discrepancy following hydrolysis. The presence of short-chain oligomers, which are rich in carbon due to their repeating units and remain soluble, could increase the measured carbon content. Additionally, the PET backsheet may contain additives or copolymers introduced to enhance material properties, which could also skew the elemental ratio. Residual EVA from the original material may further contribute to the imbalance. Peaks identified as 'Os' are attributed to the heavy metal coating applied during sample preparation for EDS analysis and are not included in the mass percentage calculations.

The similarity in recovered TPA was further confirmed through H-NMR (Fig. 10). Each spectrum displayed consistent signals, indicating that the chemical environments of the protons were alike. No large variations were observed between the products recovered using commercial ethanol and those recovered with waste ethanol. In all spectra, characteristic signals appeared at 13.31 ppm (s), 8.03 ppm (s), and at the solvent peaks for water (3.36 ppm) and DMSO (2.50 ppm). TPA contains two distinct types of hydrogen atoms: those on the carboxylic acid groups and those on the aromatic ring. Each TPA



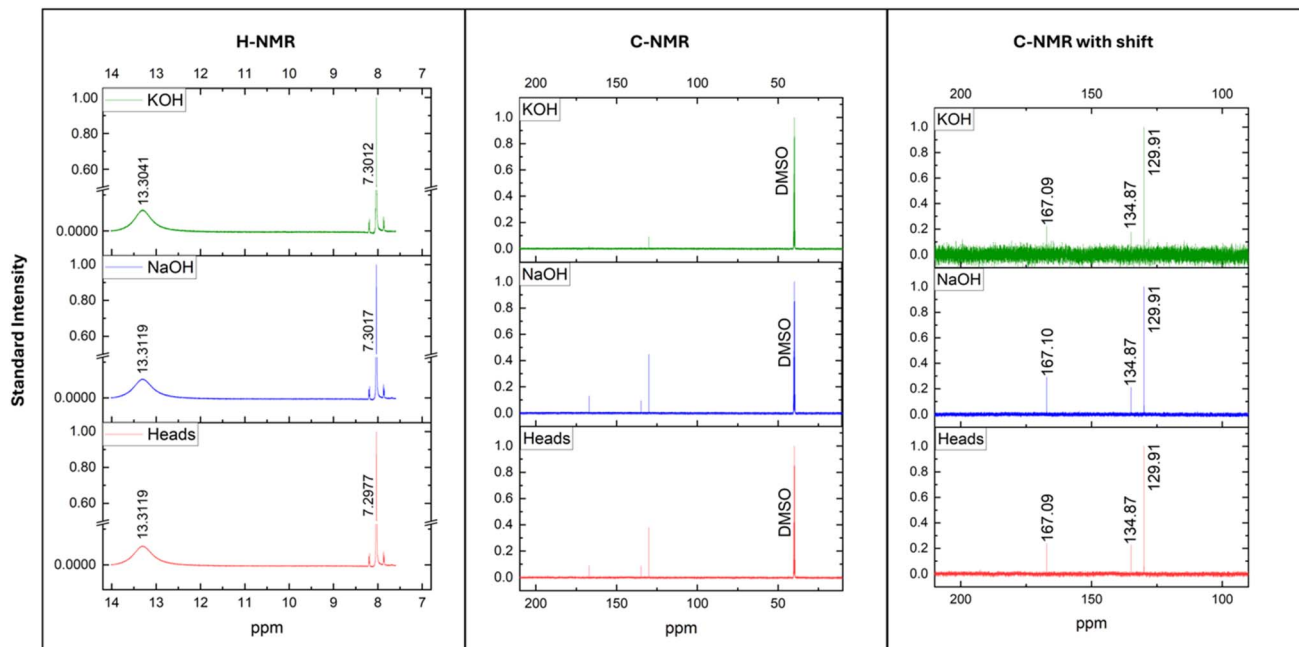


Fig. 9  $\text{H}^1$  NMR and C NMR of recovered TPA from PV backsheet.

molecule features two hydrogens on the acid groups and four on the aromatic ring, both of which are expected to produce singlet peaks, an expectation confirmed by the NMR spectra. The broad singlet at 13.31 ppm corresponds to the carboxylic acid protons (highlighted in the zoomed-in section of Fig. 10), while the singlet at 8.03 ppm corresponds to the aromatic protons on the benzene ring. No detectable impurities were present at concentrations high enough to be observed in the spectra.

In C-NMR, three peaks are observed apart from the solvent peak (DMSO), with no appreciable variation between runs. This consistency indicates that using waste ethanol in the depolymerization step does not introduce measurable variability in product quality. The three signals correspond to the expected carbon environments for a symmetric aromatic diacid: the carboxyl (carbonyl) carbons at 167.10 ppm, the ring carbons substituted by the acid groups (ipso/quaternary) at 134.87 ppm, and the remaining aromatic carbons at 129.91 ppm. Because pairs of carbons in each set are chemically equivalent, they collapse into three distinct signals.

Further, thermogravimetric analysis (TGA) of the recovered TPA products and a TPA standard shows closely similar mass-loss profiles (Fig. 10). All TPA samples exhibit the onset of oxidative mass loss at  $\sim 180$  °C, with completion by  $\sim 250$  °C, mirroring the behavior of the reference. The NaOH-derived product leaves slightly less residual ash than the KOH and ethanol-heads products; however, the differences are  $< 5$  wt% and plausibly reflect routine experimental variability (e.g., pan loading, particle size, residual moisture).

TGA traces for waste thermoform PET and the delaminated backsheet are overlaid in Fig. 10C. The indistinguishable onset temperatures, degradation rates, and residues indicate that the backsheet at this stage behaves predominantly as PET. The apparent absence of non-PET components (e.g., EVA) suggests

the backsheet can be readily routed to mixed-PET recycling streams without additional separation.

The distilled spirits sector produces a substantial ‘heads’ fraction annually, representing an under-utilized solvent pool. Substituting this stream for virgin ethanol in PET-recycling steps could lower solvent procurement and embodied impact, while avoiding disposal of the heads cut. By providing quantitative equivalence in yield and purity and a rank-ordered process window, our results support piloting in PV backsheet lines and evaluation for packaging PET where volumes are larger.

Further, the proposed workflow is tailored to PV backsheets as they have been less studied than other forms of PET, such as bottles or thermoforms, and the green process could be closely examined through the necessary delamination process and the effect of PV additives and impurities in the system. EVA swells in ethanol, resulting in low-temperature delamination, and ethanol is required for alkaline hydrolysis. Since the same solvent can be used for both steps and is used at low temperatures, examining the effects of waste solvent is essential to improve the sustainable practice of this system. In our experiments, 96.8% TPA is recovered at 8 h with NaOH with distilled heads, comparable to virgin ethanol, indicating the robustness of the process to common impurities and coatings encountered in backsheets.

However, an economic comparison between waste-derived and virgin ethanol is required for industrial decision-making. Consistent TPA yield and purity across solvent sources suggest that economics will be driven primarily by (i) solvent procurement cost, (ii) net make-up volume after recovery, and (iii) process energy. Quantifying these factors requires pilot-scale mass and energy balances and local market data; a quantitative comparison is beyond the scope of the present work. We therefore refrain from making economic claims and instead highlight these variables as priorities for future TEA.



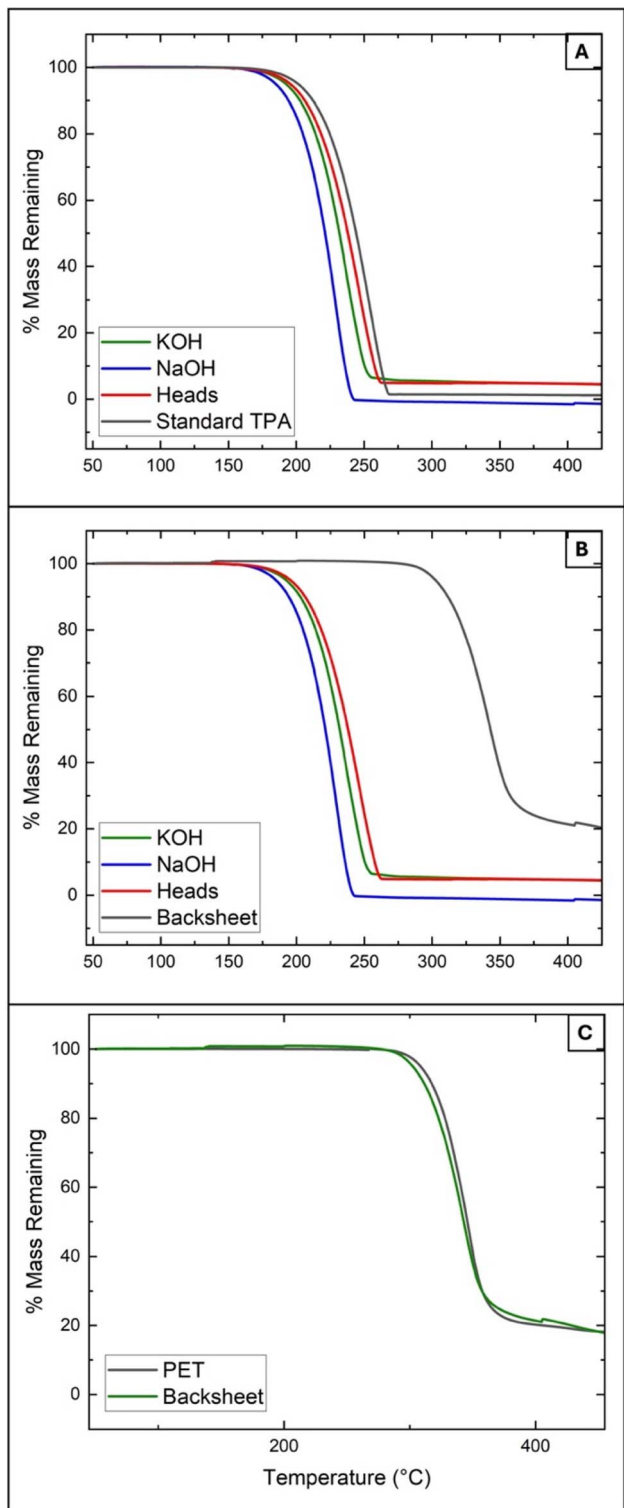


Fig. 10 Thermogravimetric analysis of the recovered TPA products with different alkalis compared to a TPA standard (A), and the original backsheets of the solar panel (B). The thermogravimetry analysis of PET and the solar panel backsheets are also compared (C).

### 3.4. Feedstock scale and applicability beyond PV backsheets

PV modules are glass-dominant devices. Polymeric content (EVA and backsheets) is typically 3–10 wt% of a c-Si module.

These materials are currently managed largely by incineration or landfilling.<sup>38</sup> At the system level, cumulative solar PV waste is projected to reach 60–78 Mt globally,<sup>39</sup> with U.S. cumulative waste 4.1 Mt by 2050. Even if only 3–10 wt% is polymeric, this corresponds to 1.8–7.8 Mt of polymers globally by 2050, still far smaller than annual global PET capacity (approximately 36 Mt per year<sup>40</sup>), dominated by packaging. Thus, PV backsheets PET waste will not drive PET recycling scale by itself; however, it represents a concentrated, regulated, and presently underserved stream where avoiding landfill/incineration offers clear environmental value and where solvent reuse can be operationalized.

Within this context, our results show that waste ethanol performs comparably to virgin ethanol for delamination/depolymerization and TPA recovery from PET-based backsheets ( $\leq 2\%$  difference in recovery in our best conditions), offering an immediately implementable route that reduces virgin solvent demand while addressing a neglected polymer fraction in PV recycling. This cross-industry coupling is independent of the absolute PET market size.

Because end-of-life PV modules are collected at central facilities, backsheets PET is geographically concentrated, facilitating solvent recovery/reuse loops. Meanwhile, the distilled-spirits “heads” stream is an available, low-value solvent by-product; valorizing it in PV/polymer operations provides a near-term circular win even if absolute PV PET tonnage is modest relative to packaging markets.

Beyond PV backsheets, the same ethanol/water-assisted alkaline depolymerization is directly applicable to single-use PET waste. Since PET ester hydrolysis governs conversion and ethanol primarily modulates mass transfer, the comparable TPA yields, and purity observed here with virgin vs. waste ethanol motivate extending the identical alkali-ethanol conditions to other PET-based waste substrates.

### 3.5. Integration within the PV recycling

Solar PV module recycling comprises: (i) mechanical removal of frames and junction boxes; (ii) recovery of glass and conductive metals/silicon from the laminate; and (iii) management of polymeric components, notably the PET-based backsheets. The waste-ethanol step demonstrated here can be effectively deployed on backsheets-rich fractions (e.g., detached backsheets or backsheets-focused cutouts) to avoid disturbing cell/metalization recovery. In practice, modules can be downsized; glass/cell laminates proceed to established delamination/metal recovery, while backsheet-rich pieces are routed to the ethanol bath and subsequent alkaline depolymerization to TPA.

The operational integration is straightforward. Covered, agitated baths with a condenser (to minimize ethanol losses) and with a simple polishing/distillation step enabling solvent recirculation can be used. The low-grade heat available at recycling facilities can supply the moderate temperatures required during delamination. This sequencing preserves yields of high-value metals/silicon and confines solvent use to the polymer stream, where it delivers the greatest benefit.



## 4. Limitations and future work

While the study presents a solvent cascading strategy to PV panel delamination and PET depolymerization using waste ethanol, several limitations remain. The manuscript does not present detailed kinetic studies for PET depolymerization or TPA hydrolysis, making it difficult to generalize reaction rates or optimize process parameters. Additionally, the presence of other organic compounds, such as methanol, in waste ethanol was not thoroughly examined, leaving uncertainties about their impact on delamination efficiency. The omission of the azeotropic behavior of ethanol–water mixtures during the reflux process is another critical gap, as it directly influences solvent stability and recovery potential. Furthermore, swelling-induced fracturing of the silicon wafer was observed, complicating the downstream recovery of valuable materials like silicon and metals.

From a methodological standpoint, the process demands sustained heating at 60–70 °C for extended periods, which could undermine the environmental benefits of using a “green” solvent like ethanol due to high energy consumption. The present work also does not address ethanol recovery, reuse potential, or waste stream treatment. In terms of industrial applicability, the techno-economic assessment of the proposed method was not done to get insights into the financial viability. The study also does not fully account for the variability in PV module composition, such as differences in EVA crosslinking or backsheet materials, which may influence the consistency and effectiveness of the process across different panel types. Together, these limitations underscore the need for further research to optimize and scale the proposed PV backsheet recovery method.

The future work in this area can focus on the following: (i) quantify PET-relevant impurity markers in recycled TPA (e.g., 4-carboxybenzaldehyde, *p*-toluic acid), (ii) conduct PET repolymerization trials using recycled and virgin TPA under identical conditions, (iii) fabricate and test PET films or backsheet laminates for dielectric strength and accelerated aging, and (iv) techno-economic analysis for industrial decision-making. These steps will link feedstock quality to end-use performance and complete the circular economy assessment.

## 5. Conclusion

This study demonstrates the effective reuse of waste solvent derived from distilled spirits production for the delamination of PET-based solar PV backsheets and the recovery of purified TPA. The process achieved delamination efficiency of 80% and a TPA recovery yield of 96.8% using waste solvent, comparable to outcomes achieved with virgin ethanol. Importantly, no degradation in the quality or purity of the recovered TPA was observed, indicating the suitability of waste ethanol as a sustainable alternative to virgin solvents. By utilizing an industrial byproduct, waste ethanol, in PV backsheet recycling, this work offers a practical and scalable example of circular economy principles in action. It not only diverts waste from the distilled spirits industry but also reduces reliance on virgin

resources and minimizes the environmental footprint of PV module end-of-life processing. Furthermore, this method requires no additional energy input or processing complexity compared to traditional approaches. However, a limitation of the current method is that a broader range of PV modules needs to be tested under varying conditions to optimize delamination and decomposition efficiencies. While the current research focused on PET-based backsheets, future investigations should expand to fluorinated backsheet materials to enable the recovery of valuable fluoropolymers alongside TPA.

In summary, our contribution is an implementation strategy that demonstrates substitution of virgin ethanol with distillery heads for PV backsheet delamination and PET depolymerization, achieving near-parity in TPA yields and product quality. Framing the work as solvent cascading clarifies the novelty as system-level and highlights a practical route to reduce virgin solvent use in PV recycling.

## Conflicts of interest

There are no conflicts to declare.

## Data availability

Additional characterization data can be found at <https://osf.io/a2c87/>  
[view\\_only=6f3de87f95184f16978b9ca93ca47a8b.](https://osf.io/a2c87/)

Supplementary information (SI) is available. See DOI: <https://doi.org/10.1039/d5su00581g>.

## Acknowledgements

This work is supported by the National Science Foundation under grant no. 2029374. We thank Dr Sachin Nimbalkar (ORNL) and Mark Robbins (ORNL) for their support in enhancing the graphics for this manuscript.

## References

- 1 International Energy Agency, Snapshot of Global PV Markets, 2024.
- 2 P. Nain and A. Anctil, End-of-life solar photovoltaic waste management: A comparison as per European Union and United States regulatory approaches, *Resour. Conserv. Recycl.*, 2024, **21**, 200212.
- 3 Y. Yu, *et al.*, Review of silicon recovery in the photovoltaic industry, *Curr. Opin. Green Sustainable Chem.*, 2023, 100870.
- 4 R. Deng, P. R. Dias, M. M. Lunardi and J. Ji, A sustainable chemical process to recycle end-of-life silicon solar cells, *Green Chem.*, 2021, **23**, 10157–10167.
- 5 P. Dias, S. Javimczik, M. Benevit and H. Veit, Recycling WEEE: Polymer characterization and pyrolysis study for waste of crystalline silicon photovoltaic modules, *Waste Manage.*, 2017, **60**, 716–722.
- 6 B. Pinlova and B. Nowack, From cracks to secondary microplastics-surface characterization of polyethylene



terephthalate (PET) during weathering, *Chemosphere*, 2024, **352**, 141305.

7 C. C. Farrell, *et al.*, Technical challenges and opportunities in realising a circular economy for waste photovoltaic modules, *Renewable Sustainable Energy Rev.*, 2020, **128**, 109911.

8 A. K. Schnatmann, F. Schoden and E. Schwenzfeier-Hellkamp, Sustainable PV module design—review of state-of-the-art encapsulation methods, *Sustainability*, 2022, **14**, 9971.

9 M. F. Azeumo, *et al.*, Photovoltaic module recycling, a physical and a chemical recovery process, *Sol. Energy Mater. Sol. Cells*, 2019, **193**, 314–319.

10 J. Tao and S. Yu, Review on feasible recycling pathways and technologies of solar photovoltaic modules, *Sol. Energy Mater. Sol. Cells*, 2015, **141**, 108–124.

11 K. J. Geretschläger, G. M. Wallner and J. Fischer, Structure and basic properties of photovoltaic module backsheet films, *Sol. Energy Mater. Sol. Cells*, 2016, **144**, 451–456.

12 L. Zhang and Z. Xu, Separating and recycling plastic, glass, and gallium from waste solar cell modules by nitrogen pyrolysis and vacuum decomposition, *Environ. Sci. Technol.*, 2016, **50**, 9242–9250.

13 J. Lee, N. Duffy, J. Petesic, T. Witheridge and J. Allen, Comparative assessment of solvent chemical delamination of end-of-life solar panels, *Waste Manage.*, 2024, **190**, 122–130.

14 P. Gangwar, N. M. Kumar, A. K. Singh, A. Jayakumar and M. Mathew, Solar photovoltaic tree and its end-of-life management using thermal and chemical treatments for material recovery, *Case Stud. Therm. Eng.*, 2019, **14**, 100474.

15 P. Su, *et al.*, Green separation and decomposition of crystalline silicon photovoltaic module's backsheet by using ethanol, *Waste Manage.*, 2024, **179**, 144–153.

16 P. J. Williams and C. R. Strauss, A treatment of grape wine distillation heads, *J. Sci. Food Agric.*, 1976, **27**, 487–498.

17 K. A. Berglund, *Artisan Distilling. A Guide for Small Distilleries*, Michigan State Univ., East Lansing, MI, 2004.

18 Distilled Spirits Council, Annual Economic Briefing, 2024.

19 N. E. Shriner, Cyclic Distillation for Energy Conservation in Spirit Production, Michigan State University, 2018.

20 J. F. Guymon, Z. Halperin and C. Crawford, Methods of Treating or Processing Heads & Principles or Fusel Oil Separation during Distillation a Seminar, *Am. J. Enol. Vitic.*, 1950, **1**, 86–100.

21 P. Godden and M. Gishen, The trends in the composition of Australian wine from vintages 1984 to 2004, *Aust. N. Z. Wine Ind. J.*, 2005, **20**, 21.

22 M. C. CRUZ, Tequila production from agave: historical influences and contemporary processes, *The Alcohol Textbook*, 223, 2003.

23 P. W. Madson, Ethanol Distillation: The Fundamentals, *The Alcohol Textbook*, 2003.

24 R. Pigget, Production of heavy and light rums: Fermentation and maturation, *The Alcohol Textbook*, 2003, 246–253.

25 T. P. Lyons Production of Scotch and Irish whiskies: Their history and evolution, *The Alcohol Textbook*, ed. Jacques K. A., Lyons T. P. and Kelsall D. R., 4th edn, 2003, 193–222.

26 R. Hardian, A. Gaffar, C. Shi, E. Y.-X. Chen and G. Szekely, Chemically recyclable nanofiltration membranes fabricated from two circular polymer classes of the same monomer origin, *J. Membr. Sci. Lett.*, 2024, 100067.

27 H. Hu, Y. Wu and Z. Zhu, Optimization of microwave-assisted preparation of TPA from waste PET using response surface methodology, *J. Polym. Environ.*, 2018, **26**, 375–382.

28 K. Lee, Y. Jing, Y. Wang and N. Yan, A unified view on catalytic conversion of biomass and waste plastics, *Nat. Rev. Chem.*, 2022, **6**, 635–652.

29 L. Yuan, P. Nain, M. Kothari and A. Anctil, Material intensity and carbon footprint of crystalline silicon module assembly over time, *Sol. Energy*, 2024, **269**, 112336.

30 Y. He, H. Ke and Y. Lu, Alcoholytic of ethylene-vinyl acetate copolymer catalyzed by alkaline: A kinetic study based on in situ FTIR spectroscopy, *Chem. Eng. J.*, 2023, **464**, 142695.

31 X. Xue, L. Tian, S. Hong, S. Zhang and Y. Wu, Effects of composition and sequence of ethylene-vinyl acetate copolymers on their alcoholytic and oxygen barrier property of alcoholyzed copolymers, *Ind. Eng. Chem. Res.*, 2019, **58**, 4125–4136.

32 C. Hirschl, *et al.*, Determining the degree of crosslinking of ethylene vinyl acetate photovoltaic module encapsulants—A comparative study, *Sol. Energy Mater. Sol. Cells*, 2013, **116**, 203–218.

33 K. P. R. Chowdary and J. S. Babu, Permeability of ethylene vinyl acetate copolymer microcapsules: Effect of solvents, *Indian J. Pharm. Sci.*, 2003, **65**, 62–66.

34 H. K. Trivedi, A. Meshram and R. Gupta, Removal of encapsulant Ethylene-vinyl acetate (EVA) from solar cells of photovoltaic modules (PVMs), *Mater. Today: Proc.*, 2023, 73–76.

35 W.-Y. Chuang, T.-H. Young, D.-M. Wang, R.-L. Luo and Y.-M. Sun, Swelling behavior of hydrophobic polymers in water/ethanol mixtures, *Polymer*, 2000, **41**, 8339–8347.

36 S. X. Chen and R. T. Lostritto, Diffusion of benzocaine in poly (ethylene-vinyl acetate) membranes: Effects of vehicle ethanol concentration and membrane vinyl acetate content, *J. Controlled Release*, 1996, **38**, 185–191.

37 H. K. Trivedi, R. K. Yadav, A. Meshram and R. Gupta, Removal of encapsulant ethylene-vinyl acetate for recycling of photovoltaic modules: Hansen solubility parameters analysis, *Process Saf. Environ. Prot.*, 2024, **186**, 1397–1409.

38 P. Nain and A. Anctil, End-of-life solar photovoltaic waste management: A comparison as per European Union and United States regulatory approaches, *Resour. Conserv. Recycl.*, 2024, **21**, 200212.

39 UMSICHT, F, End-of-life pathways for photovoltaic backsheets, Retrieved April 5, 2022, 2017.

40 Global Data, Polyethylene Terephthalate (PET) Industry Capacity and Capital Expenditure Forecasts with Details of All Active and Planned Plants to 2028, 2024.

